



Performance and Reuse of Steel Shot in Abrasive Waterjet Cutting of Granite

Yohan Cha¹ · Tae-Min Oh² · Gun-Wook Joo³ · Gye-Chun Cho⁴

Received: 15 July 2020 / Accepted: 28 November 2020 / Published online: 3 January 2021
© The Author(s) 2021

Abstract

Steel shots are suitable for abrasive waterjet rock cutting and recycling because of the high hardness and magnetic properties of steel. This study evaluated the rock-cutting performance and recycling characteristics of steel shot waterjet. The rock-cutting responses of steel shot and garnet were compared at the same waterjet conditions. The used steel shot was collected and the particle-size changes were evaluated before reuse, and its cutting performance was re-evaluated. Overall, the steel shot waterjet yielded improvements in performance in the range of 30–50% compared with the garnet waterjet. Moreover, the recycled steel shot yielded a 50% reduction in cutting performance. Rust was observed on the surface of the used steel shot, the used steel shots were partially destroyed, and the debris on the abrasive surface needed to be removed by drying. The reusable steel shot left on the 80th sieve converged to 60% in each recycling run. The results of this study can be used to reduce the cost of abrasive waterjet and industrial waste.

Keywords Abrasive waterjet · Steel shot · Abrasive recycling · Rock cutting

List of Symbols

C_c	Coefficient of gradation	d_p	Diameter of abrasive particle (mm)
C_u	Uniformity coefficient	E_e	Effective erosion kinetic energy (J)
D	Cutting depth (mm)	E_p	Abrasive kinetic energy (J)
D_{10}	Effective particle size (mm)	H_p	Hardness of particle, Knoop (kg/mm ³)
D_{50}	Mean particle size (mm)	H_t	Hardness of target rock, Knoop (kg/mm ³)
D_{max}	Maximum cutting depth (mm)	m_p	Single-particle mass (g)
		\dot{m}_a	Abrasive flow rate (g/s)
		$\dot{m}_{a(op)}$	Optimum abrasive flow rate (g/s)
		\dot{m}_w	Water flow rate (ml/s)
		N_p	Number of abrasive particle
		p_c	Threshold pressure (MPa)
		t	Operating time
		v_a	Velocity of abrasive particle (m/s)
		v_r	Removed volume by the single abrasive particle (mm ³)
		V_r	Total cutting volume (mm ³)
		v_t	Terminal velocity (m/s)
		v_w	Velocity of fluid (m/s)
		$v_{w,o}$	Velocity of water in the orifice section (m/s)
		η_t	Momentum transfer parameter
		ρ_p	Particle density (g/mm ³)
		S_f	Fresh steel shot
		S_{R1}	Recycled once steel shot
		S_{R2}	Recycled twice steel shot
		S_{R3}	Recycled three times steel shot
		SOD	Standoff distance (mm)

✉ Gye-Chun Cho
gyechun@kaist.edu

Yohan Cha
ycha@kimga.re.kr

Tae-Min Oh
geotaemin@pusan.ac.kr

Gun-Wook Joo
clucio@add.re.kr

¹ Geologic Environment Division, Deep Subsurface Research Center, Korea Institute of Geoscience and Mineral Resources (KIGAM), Daejeon 34132, Republic of Korea

² Department of Civil Engineering, Pusan National University (PNU), Pusan 46241, Korea

³ The 4th R&D Institute-3rd Directorate, Agency for Defense Development (ADD), Daejeon 16545, Korea

⁴ Department of Civil and Environmental Engineering, Korea Advanced Institute of Science and Technology (KAIST), Daejeon 34141, Republic of Korea

1 Introduction

Abrasive waterjets are extensively used in a variety of industrial applications for cutting materials, such as metals, alloys, rock, and exotic materials. The use of abrasives in waterjets is a key aspect of the cutting target process with acceleration-dependent energy (Momber 2004; Oh and Cho 2013; Zeng and Kim 1996). However, the cost of abrasives is ~ 60% of the total cost (Hashish 2011). Increased abrasive consumption and its cost are one of the limitations of the waterjets. Therefore, the introduction and use of more economical technologies is a challenge.

Various attempts have been expended to reduce the cost by improving the use of abrasives. Table 1 summarizes the literature on abrasive recycling for waterjets. Recycling abrasives reduce the overall cost and are environmentally friendly (Babu and Chetty 2003; Chetty and Babu 1999). As a result, studies on the effects of particle size on garnet recycling have led to the conclusion that abrasives with sizes of 90 μm or less are not suitable for recycling. Furthermore, the larger the abrasive is, the more efficient it is for recycling (Guo et al. 1992). A study was conducted on the cutting performance according to the mixing ratio of the recycled abrasive and the deformation characteristics of the particles. The mixing ratio of the optimum recycled abrasive has been suggested to be 40% (Babu and Chetty 2002). Performance degradation owing to repeated abrasive recycling has also been investigated. Accordingly, it

has been confirmed that the performance is reduced by ~ 20% per recycling run during the final four recycling runs (Babu and Chetty 2003). In particular, studies on recycling garnet for rock cutting showed the possibility of reuse of abrasives for geotechnical purposes. The recycling rate of garnet used for granite cutting decreased by 82%, 28%, 34%, and 18% with increasing recycling runs, and a limitation of three rounds of recycling was suggested considering the disintegration of garnet (Aydin 2015). The cutting results of various types of granite showed a strong correlation between the recycling rate and the micro-hardness (Aydin 2014). The black granite cutting depth of recycled garnet was 48–79% of fresh garnet, but the surface finish was improved owing to the finer and improved roundness of the used garnet (Chetty and Babu 1999). Conversely, ductile material cutting performance of recycled garnet showed higher than fresh garnet. At this time, the recycling rate was ~ 58% (Pi 2008; Pi et al. 2013). The experiment of abrasive particle disintegration used in waterjet indicated that almost 50% of the garnet was reusable (Perec 2017).

For garnets, which are the most common abrasives, the processes of collection and treatment for recycling are complicated and have high cost. In this regard, steel shots are suitable for abrasive recycling. Steel shots are the heavy materials with high density. Thus, they have low-destruction rates and dust. Steel is easy to collect based on the magnetic properties in recycling. High-recycling rates are expected to be more economical owing to the reduced environmental wastage and

Table 1 Literature review of abrasive recycling for waterjet

Abrasive type	Investigation/observation	References
Garnet	The cutting efficiency and recovery of recycling garnet was studied; the cutting depth of recycled garnet ranged from 48 to 79%, and the surface finish was found to have improved with recycled abrasive	Chetty and Babu (1999)
Garnet	Changes in reusability of garnets between fresh garnets and those recycled three times on ductile material cuttings were discussed. Reusable garnet of over 90 μm yielded ranges in the order of 83%	Babu and Chetty (2003)
Garnet	The characteristics of abrasive recharging were reported; the optimized abrasive mixing rate was 40% of recycled garnet on ductile material cutting	Babu and Chetty (2002)
Garnet	The recycling capacity of the abrasive was discussed as a function of disintegration; the particle size of recycled abrasives increased and was affected by the conditions of the focus diameter	Guo et al. (1992)
Garnet	The cutting performance of recycled garnet for ductile materials was tested; the cutting depth of recycled garnet was higher than that of fresh garnet	Pi (2008)
Garnet	Recycle characteristics of the garnet in waterjet machining were investigated; the reusability of garnet was 58.86%, and the optimum particle size for recycling was higher than 90 μm	Pi et al. (2013)
Garnet and corundum	Abrasive disintegration and recycling possibility were tested; almost 50% of the garnet and 47–67% of corundum could be reused	Perec (2017)
Garnet	Garnet recycling in rock cutting was investigated; the reusability was reduced by 82%, 58%, 34%, and 18% during recycling runs due to disintegration	Aydin (2015)
Garnet	Recycling was evaluated for different types of granite; a strong correlation between cutting performance and micro-hardness was observed	Aydin (2014)

reduced environmental costs. The properties of steel shot (used as abrasives), including size, roundness, density, and sphericity of steel shot and steel grit, are thus introduced and discussed. The roundness was used for particle velocity prediction (Hashish 1989). The increased kinetic energy of a single steel shot is more suitable for cutting brittle materials. Based on these characteristics, a theoretical consideration of the abrasive acceleration has been considered (Galecki and Summers 1992; Summers 2003). The specific energy of the steel ball and other abrasives, such as tungsten carbide and Ottawa sand, were calculated for Indiana limestone drilling, and their performances were evaluated (Maurer and Joe 1969). Based on the same principles, a study on the peening performance and resulting surface roughness was conducted with steel balls to evaluate the feasibility of the steel ball abrasive (Daniewicz and Cummings 1999; Fowler et al. 2009; Salko 1984).

As described above, various approaches have been tested on steel shot for abrasives, but studies on the steel shot waterjet for rock cutting have been limited. In addition, targeted studies on steel shot recycling with abrasive waterjets are still lacking. For economical uses of steel shots in geotechnical purpose, it is necessary to compare the performance differences between the steel shot and garnet for rock cutting. Correspondingly, the practicality of recycling needs to be verified. Therefore, in this study, experiments were conducted on the rock-cutting performance and recycling characteristics of steel shot. The effects of energy (i.e., the water pressure, abrasive flow rate, and traverse speed), and geometric parameter (i.e., the stand-off distance) were assessed based on the cutting performance measurements (depth, width, and volume of cut) of the steel shot and garnet. To evaluate the recycling characteristics of the steel shot for rock cutting, used steel shots were collected after use, and recycling was repeated up to three times. The steel shot was subjected to a particle distribution analysis based on their reuse, and the surface condition was observed by macrophotography. As a result of this study, the rock-cutting performance was evaluated as a function of the various waterjet parameters. Furthermore, the recycling characteristics of the steel shot, such as the surface conditions, changes of the particle-size distribution, and reused cutting rate, were reviewed based on the recycling number. In conclusion, steel shot exhibited an improved cutting efficiency than the garnet, and was the best option for recycling abrasive. Conversely, to prevent deterioration attributed to repeated recycling cycles, surface treatments of steel shots and size classification after collection were necessary.

2 Theoretical Background

2.1 Effective Erosion Kinetic Energy

The abrasive serves the main energy source in abrasive waterjet rock cutting, according to its velocity (v_a) and mass (\dot{m}_a). (Finnie 1960; Jankovic et al. 2013; Momber 2001). The abrasive is accelerated by the high-velocity water flow ($v_{w,o}$) produced by the high-pressure water pump (Momber and Kovacevic 2012). The momentum of the high-velocity water flow ($\dot{m}_w \times v_w$) is transferred to the momentum of the abrasive ($\dot{m}_a \times v_a$). This transfer continues until the terminal velocity (v_t) of water and abrasive becomes equal (Cha et al. 2020; Momber and Kovacevic 2012):

$$\dot{m}_w v_{w,o} = \dot{m}_w v_w + \dot{m}_a v_a = (\dot{m}_w + \dot{m}_a) v_t, \quad (1)$$

where \dot{m}_w is the water flow rate, $v_{w,o}$ is the velocity of water at the pump, v_w is the velocity of water during acceleration, \dot{m}_a is the abrasive flow rate, and v_a is the velocity of abrasive during acceleration. The abrasive acceleration and mixing efficiency are expressed in terms of a momentum transfer parameter (η_t) that is affected by the abrasive flow rate, and determines the terminal velocity (Cha et al. 2020; Momber and Kovacevic 1995; Oh and Cho 2015):

$$v_t = \eta_t \frac{v_{w,o}}{1 + (\dot{m}_a/\dot{m}_w)}. \quad (2)$$

The waterjet abrasive has kinetic energy (E_p) depending on its terminal velocity and mass:

$$E_p = \frac{1}{2} \dot{m}_a v_t^2 t = \frac{1}{2} \dot{m}_a \left(\eta_t \frac{v_{w,o}}{1 + (\dot{m}_a/\dot{m}_w)} \right)^2. \quad (3)$$

Given that the energy conversion of the accelerated abrasive depends on the hardness relationship between the abrasive and the object to be cut, the effective erosion kinetic energy (E_c) is expressed based on the consideration of the hardness relationship, as follows (Vahedi Tafreshi and Pourdeyhimi 2003; Zhu et al. 2009):

$$E_c = \frac{E_p}{1 + \sqrt{H_t/H_p}} = \frac{\dot{m}_a \cdot t}{2(1 + \sqrt{H_t/H_p})} \cdot \left(\eta_t \frac{v_{w,o}}{1 + (\dot{m}_a/\dot{m}_w)} \right)^2, \quad (4)$$

where H_t and H_p represent the hardness of the target rock and particle, respectively.

Based on the theoretical approach of energy conservation, the effective erosion kinetic energy is expended to remove materials (Capello and Groppetti 1993; El-Domiatiy and Abdel-Rahman 1997; Zeng and Kim 1992; Zeng and Kim 1996):

$$\frac{dv_r}{dt} = \frac{dE_e}{dt}, \quad (5)$$

where v_r is the removed volume by the single abrasive particle, and t is time.

The eliminated target volume is represented by the relationship between the work expended by the abrasive to the final depth of the abrasive indentation owing to the material hardness (Cha et al. 2019). The removed volume is proportional to the diameter (d_p), velocity (v_t), density (ρ_p), and hardness (H_p) of the abrasive:

$$v_r \propto \frac{d_p^3 \cdot v_t^3 \cdot \rho_p^{1.5}}{\left(H_t \left(1 + \sqrt{H_t/H_p}\right)\right)^{1.5}}. \quad (6)$$

2.2 Number of particles and erosion volume

The number of injected abrasive particles (N_p) can be represented by the mass of the abrasive input per time, the mass of a single abrasive particle (m_p), and waterjet operating time (t):

$$N_p = \frac{\dot{m}_a}{m_p} \cdot t. \quad (7)$$

It is expressed in terms of the diameter (d_p) and density (ρ_p) of the single abrasive particle:

$$N_p = 6 \frac{\dot{m}_a}{\pi d_p^3 \rho_p} \cdot t. \quad (8)$$

By calculating the material removal volume by a single abrasive and the number of abrasive input, the total cutting volume (V_r) is given as follows:

$$V_r = v_r \cdot N_p. \quad (9)$$

Substituting Eqs. (6) and (8) into Eq. (9), the removal volume of the input abrasives can be expressed as a function of abrasive properties and target hardness, as shown below:

$$V_r = v_r \cdot N_p \propto \frac{6 \cdot v_t^3 \cdot \rho_p^{0.5} \cdot \dot{m}_a}{\pi \left(H_t \left(1 + \sqrt{H_t/H_p}\right)\right)^{1.5}} \cdot t. \quad (10)$$

In this case, the cutting performance is determined by the hardnesses and densities of each abrasive type with the same input mass of steel shot and garnet. This theoretical result is discussed in the experimental section.

Table 2 Steel ball properties

Rock type	Steel shot	Garnet
Hardness		
(Hv)	1500	1350
(Mohs)	8.2	6.5
Weight density (g/cm ³)	7.78	3.93
Mean diameter (mm)	0.18	0.18
Young's modulus (GPa)	100.2	68
Component	C, Mn, Si, S, P	Mg ₃ Al ₂ (SiO ₄) ₃



Fig. 1 Abrasives for experiment: steel shot and garnet

3 Experimental Program

3.1 Abrasives and Rock Properties

The rock-cutting performances of the steel shot and garnet were evaluated at the same waterjet parameter conditions, such as the pump pressure, traverse speed, abrasive flow rate, and standoff distance (SOD). The steel shot used after the experiment was collected to test reusability.

Table 2 lists a summary of the abrasive properties. The chemical analysis revealed that the steel shots contained 0.8–1.2 of carbon, 0.35 manganese, 0.4 of silicon, 0.05 sulfur, and 0.05 phosphorus [all values expressed in the percentage by mass (WT %)]. The steel shot had a higher hardness than that of the garnet of [i.e., 8.2 of the Mohs' hardness (HM)], and had a specific gravity that was approximately twice as that of the garnet (i.e., 7.78). The intensifier waterjet system was supplied with the commercial mesh size grade in the range of 60–80 (diameter of 0.18–0.22 mm) steel shot and garnet (Fig. 1). The size of the abrasives were prepared in a similar manner in a comparative study on the garnet recycling characteristics based on the mesh size of 80 (Babu and Chetty 2003). The steel shot used in experiments was mostly steel ball mixed with a small amount of angled-steel grit.

Table 3 Specimen properties

Rock type	Granite
Weight density (g/cm ³)	2.58
Porosity (%)	0.68
Compressive strength (MPa)	208.5
Tensile strength (MPa)	10.2
Young’s modulus (GPa)	30.2
P-wave velocity (m/s)	3394
International Society for Rock Mechanics Classification	Very strong rock

The rock specimen chosen was of granite, considering the practical applications of geotechnical abrasive waterjets. In Korea, granite is the most typical rock that is encountered in construction sites. The size of the specimens was 200 mm × 200 mm × 300 mm, and all the specimens were from the same depth and from the same location in the Hwangdeung region for property unification. The specimens had a density of 2.58 g/cm³, porosity of 0.68%, and uniaxial compressive and tensile strengths of 208.5 MPa and 10.2 MPa, respectively, and a P-wave velocity of 3394 m/s. The properties of rock specimens were estimated based on the guidelines of the International Society for Rock Mechanics [ISRM; (ASTM 2014; Brown 1981)]. The relevant details of the rock specimens are listed in Table 3.

3.2 Test Parameters for Rock Cutting

Experiments were conducted by varying the energy parameters (i.e., water pressure, abrasive flow rate, and traverse speed), and the geometric parameter (i.e., the standoff distance) for performance comparisons with the system and operational conditions. The effects of the energy parameters were evaluated based on the application of water pressure at 157, 235, and 314 MPa, the use of traverse speeds of 1.9, 8.4, and 14.1 mm/s, and the variation of the abrasive flow rate from 0 (plain waterjet) to 44.75 g/s. To assess the effects of the geometric parameter, the standoff distances were set to 10, 100, and 200 mm. The steel shot reusability were tested at a water pressure of 235 MPa and the traverse speed was set to 8.4 mm/s, while all the other experimental conditions were maintained the same. Test cases for fresh steel shot are listed in Table 4, and test cases for recycled steel shot are listed in Table 5.

3.3 Test Setup and Experimental Testing Procedures

A typical abrasive waterjet system is shown in Fig. 2. The force of the water stream accelerates the abrasives, and the orifice diameter and pump pressure are among the most important factors responsible for the water flow rate. For the experiment, a 50 hydraulic power intensifier pump was used. This pump can produce a maximum pressure of 420 MPa and a maximum water flow rate of 6 l/m. The abrasive injection waterjet type (AWJ, conventional abrasive jetting) was used. The nozzle head system consisted of the sapphire orifice (diameter: 0.254 mm), and a tungsten carbide focus (diameter: 0.76 mm,

Table 4 Test cases for fresh steel shot

	S_f									
Abrasive type	Fresh steel ball (S_f) and garnet									
Water pressure (MPa)	314	235			157					
Water flow rate (ml/s)	28.3	24.5			20.0					
Abrasive flow rate (g/s)	7.36–44.75	10.35–21.13			11.5–19.85					
Standoff distance (mm)	10	100	200	10	100	200	10	100	200	
Traverse speed (mm/s)	1.9	1.9	1.9	1.9	1.9	1.9	1.9	1.9	1.9	1.9
	8.4	8.4	8.4	8.4	8.4	8.4	8.4	8.4	8.4	8.4
	14.1	14.1	14.1	14.1	14.1	14.1	14.1	14.1	14.1	14.1

Table 5 Test cases for recycled steel shot

	S_{r1}				S_{r2}				
Abrasive type	Steel ball used once before (S_{r1})				Steel ball used twice before (S_{r2})				
Water pressure (MPa)	235				235				
Water flow rate (ml/s)	28.3				24.5				
Abrasive flow rate (g/s)	7.22–27.96				8.89–12.19				
Standoff distance (mm)	10	100	200	10	100	200	10	100	200
Traverse speed (mm/s)	8.4	8.4	8.4	8.4	8.4	8.4	8.4	8.4	8.4

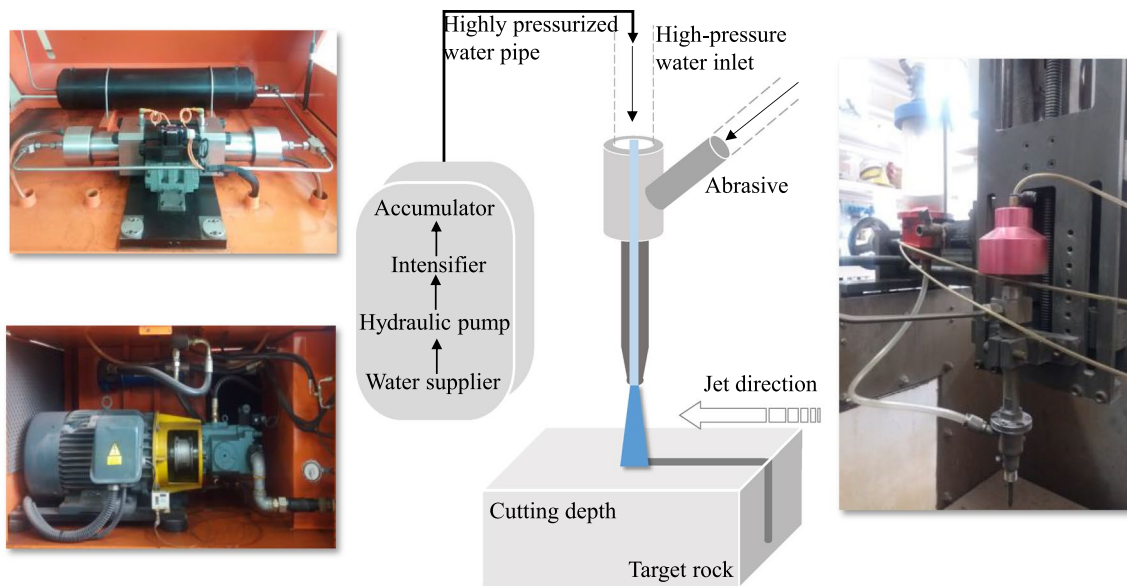


Fig. 2 Diagram of the waterjet system used in the experiment

length: 76.2 mm). The jetting moved once in one direction, and the performance was evaluated based on the measurements of the cutting depth and volume. These were measured at least three times, and the average value was obtained. The cutting volume was measured by pouring water in the cutting space. These cutting results were compared with those of the garnet.

After cutting the rock with fresh steel shot, used abrasives were collected and dried to test the performance of the recycled steel shot. Furthermore, the steel shot particle-size distribution was evaluated with fresh steel shot (S_f), and with recycled steel shot that was recycled once (S_{R1}), twice (S_{R2}), and three times (S_{R3}) during the abrasive waterjet rock-cutting process. Dry sieve tests for particle-size distribution were based on the American Society for Testing Materials (ASTM) standard test method D422-63 (ASTM 2007) and D6913-04 (ASTM 2009). To determine the reusable steel shot rate for recycling, the same size as that collected for fresh steel shot was collected with the mesh sizes between 60 and 80. To prevent rusting, the used steel shots were dried in an oven at 70 °C. Some of the used abrasives were naturally dried at 21 °C (room temperature) to evaluate the effect of the drying conditions. The surfaces of recycled particles were observed with an optical microscope (Mitutoyo, 10×M plan Apo) and a personal computer (PC) camera (Moticam 2300) in each recycling process.

4 Steel Shot and Garnet Waterjet Granite Cutting Performances

4.1 Water Pressure Effects

The rock-cutting outcomes of an abrasive waterjet depend on the abrasive type and waterjet parameters. As shown in Fig. 3, the cutting path on the rock specimens space out without affecting each other. Figure 4 shows the cutting depth that depended on the water pressure at a standoff distance of 10 mm. At the tested conditions, the cutting depths of steel shot were ~ 30–40% deeper than those of the garnet. For each traverse speed, the cutting depth linearly increased as a function of pressure. The increase in the pressure increased the velocity of the high-pressurized water that yielded a higher abrasive energy that led to an improved cutting performance. The threshold pressure (p_c , minimum critical pressure) was required to cut the granite (Evans et al. 1978; Oh and Cho 2013), and ranged from 80 to 100 MPa regardless of the abrasive type. This threshold pressure depended on the properties of the cutting material.

Figure 5 shows the cutting results owing to the water pressure at various traverse speeds. This parameter

Fig. 3 Results of an abrasive waterjet rock cutting with abrasive type and waterjet parameters

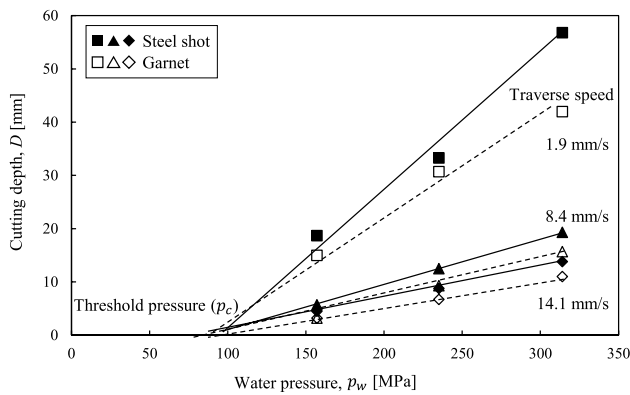
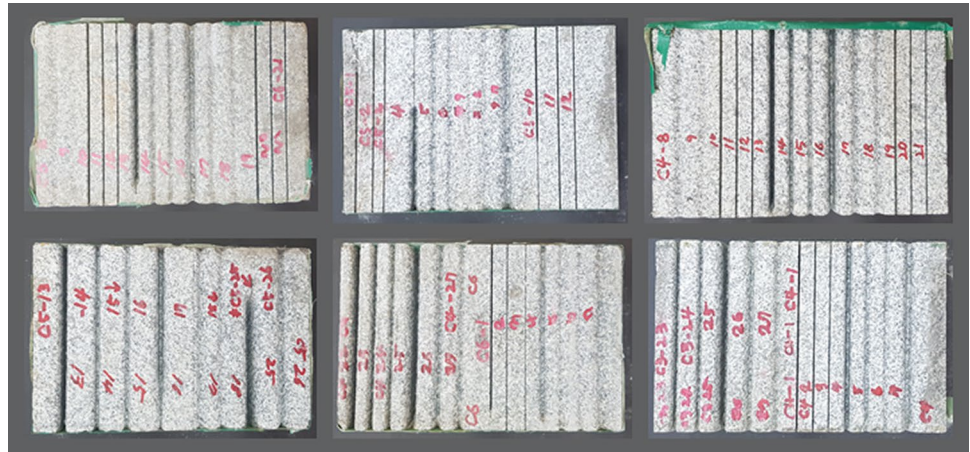


Fig. 4 Effects of the water pressure on the cutting depth using a steel ball

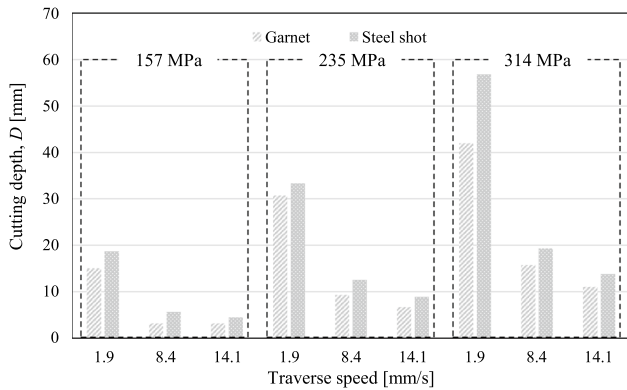


Fig. 5 Effects of the traverse speed on the cutting depth

indicates the exposure time of the waterjet energy that was intended to be cut (Ay et al. 2010; Hascalik et al. 2007). As observed, the cutting depth increased owing to the accumulated energy at slow traverse speeds. In the cases of the garnet and the steel shots, the higher the exposure

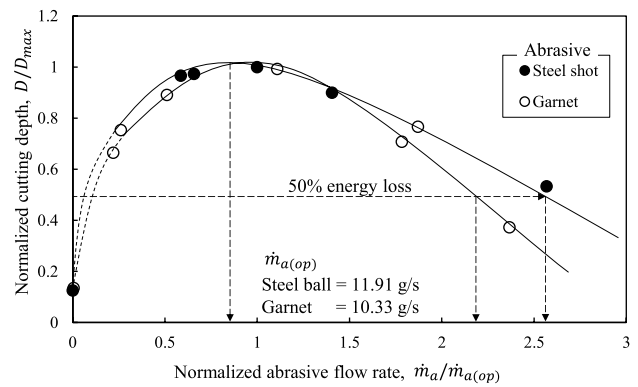


Fig. 6 Abrasive flow rate and rock-cutting depth using steel ball and garnet

time of jet energy (i.e., slower traverse speeds), the greater the effects of the water pressure.

4.2 Abrasive Flow Rate Effects

Given that the momentum of the water was converted to the momentum of the abrasive during mixing and acceleration, the abrasive flow rate in an AWJ determined the velocity and energy of the abrasive (Eq. 3). As the abrasive flow rate increased, the cutting performance increased as the number of abrasive particles (e.g., impact frequency) increases as a function of energy. However, beyond a specific abrasive flow rate (i.e., optimum abrasive flow rate, $\dot{m}_{a(op)}$), the cutting performance decreased owing to the reduction of the mixing efficiency and terminal velocity (Eq. 2). Figure 6 shows the cutting depth (D) and abrasive flow rate (\dot{m}_a) of the steel shot and garnet in the same waterjet system configuration. Each result was normalized based on the maximum cutting depth (D_{max}) and optimum abrasive flow rate ($\dot{m}_{a(op)}$). The maximum cutting depth with the steel shot was achieved at the abrasive flow rate of 11.91 g/s, that is, at the optimum

Fig. 7 Effects of the standoff distance on the cutting depth

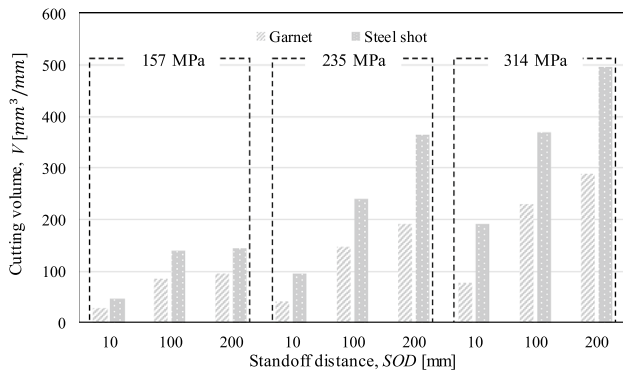
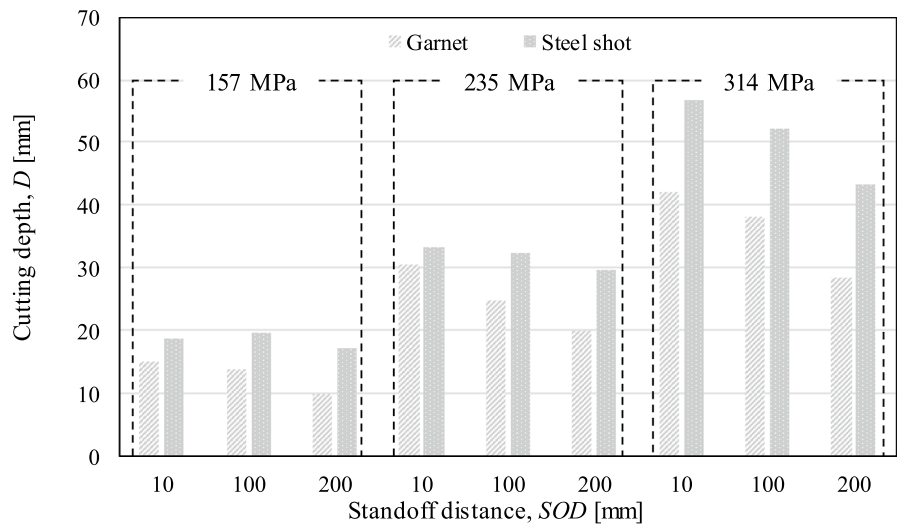


Fig. 8 Effects of the standoff distance on the cutting volume

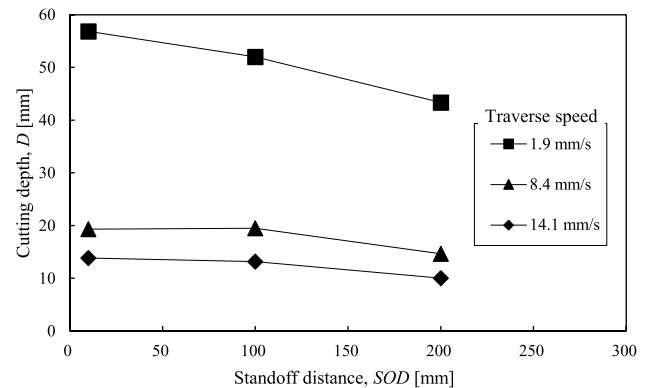


Fig. 9 Effects of the traversal speed and SOD on the cutting depth of the steel shot

abrasive flow rate of the steel shot, and at the flow rate of 10.33 g/s in the case of the garnet, which was 40.3% of the mass ratio of the water flow rate (\dot{m}_w). Owing to the fact that the energy transfer of the high-velocity water to the abrasives depends on the input mass regardless of the abrasive density and the number of particles, the normalized depth of cut and abrasive flow rate by steel shot and garnet are similar.

4.3 Standoff Distance Effects

The waterjet cutting for geotechnical purposes requires greater depths and widths than roughness and quality. Therefore, the standoff distance becomes one of the main variables. Geotechnical use of waterjets is necessary to set a high-standoff distance to obtain the greater cutting volume. The cutting results shown in Figs. 7 and 8 indicate that as the standoff distance increases, the cutting depth decreases as the concentrated energy decreases. However, the cutting volume increases owing to the cutting width increments.

These results demonstrate that the larger the standoff distance is, the better the performance is in terms of the material volume removal. However, in the case of the waterjetting method that assisted mechanical excavation, small standoff distances are suitable for deeper cutting depths. The results indicate the increased cutting performance with the use of steel shot compared with garnets, the steel shot led to better volume cutting performances than those of the garnet by approximately 40–50%. The volume removal ratio for each abrasive can be expressed from Eq. (10) as a function of the abrasive density, hardness, and the removal material hardness as follows:

$$V_{rs}/V_{rg} \propto \sqrt{\rho_s^{0.5}/\rho_g^{0.5}} \left(\frac{1 + \sqrt{H_t/H_g}}{1 + \sqrt{H_t/H_s}} \right)^{1.5} \quad (11)$$

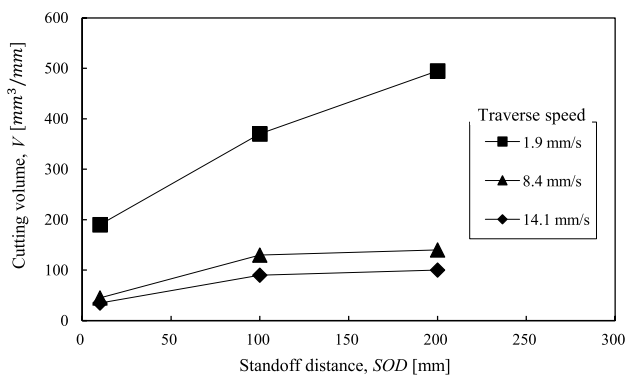


Fig. 10 Effects of the traversal speed and SOD on the cutting volume of the steel shot

According to the density and hardness of the steel shot and the garnet used in experiment (Table 1 ie., with densities of 7.78 and 3.93 g/cm³, and hardnesses of 8.2 and 6.5 Hv), the volume removal ratio is 1.402. Based on this theoretical approach, the steel shot has a 40.2% higher cutting performance than that of the garnet has.

Figures 9 and 10 show the effects of the standoff distance as a function of the traverse speed. The difference in the cutting depth could explain the fact that the slow traverse speed was affected considerably by the standoff distance. The traverse speed was a function of the time the rock specimen was exposed to the abrasive energy, and the standoff distance was a function of the density of the energy. Therefore, these results are the general relationship between cutting efficiency as a function of energy density and exposure time.

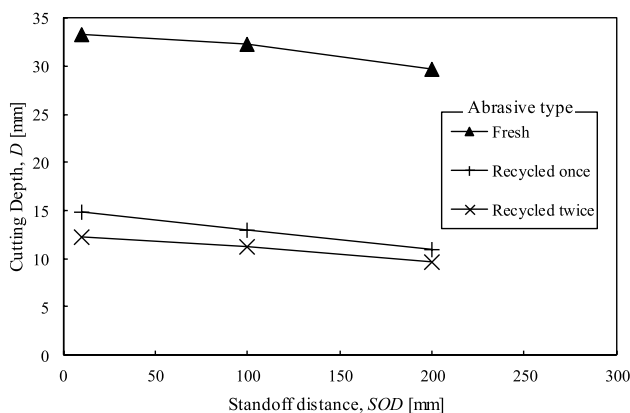


Fig. 11 Effects of the recycling times on the cutting depth using fresh steel and recycled steel shot

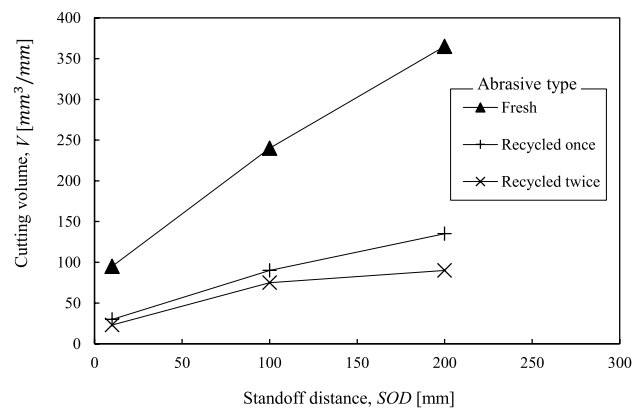


Fig. 12 Effects of the recycling times on the cutting volume using fresh and recycled steel shot

5 Recycle Characteristics of Steel Shot Waterjet

5.1 Cutting Performance of Recycled Steel Shot

Figures 11 and 12 show the cutting performances of fresh steel shot after one or two cycle runs as a function of the SOD. The cutting performance of the steel shot that was recycled once was ~ 50% of that of fresh steel shot. The results obtained from steel shots that were recycled twice were similar with those of the steel shots that were recycled once but their values were slightly lower.

5.2 Particle-Size Characteristics of Recycled Steel Shots

On the surface of the steel shot before drying, a lot of debris of the broken steel shot was observed. However, after oven drying, the surface debris was removed naturally, as shown in Fig. 13. To use recycled steel shot for the injection waterjet system as well as the suspension waterjet, the recycled steel shot needed to be dried. Therefore, the collected steel shot was observed after drying.

Figure 14 shows the size distribution of fresh and recycled steel shot obtained by sieve analysis. Using these results, to evaluate the changes in particle sizes, the effective size (D_{10} : diameter corresponding to 10% finer), mean particle size (D_{50} : diameter corresponding to 50% finer), uniformity coefficient (C_u : D_{60}/D_{10}), and coefficient of gradation (C_c : $D_{30}^2/[D_{60} \times D_{10}]$) were determined, as shown in Fig. 15.

After a single use of the fresh steel shot for rock cutting, the steel shot particles were destroyed and disintegrated (i.e., D_{50} and D_{10} were reduced, and C_u increased). As shown in Fig. 16, broken particles were observed at the mesh size 100. A slight rust was observed on the surface of the used steel shot which maintained the spherical shape.

Fig. 13 Used steel ball before and after drying

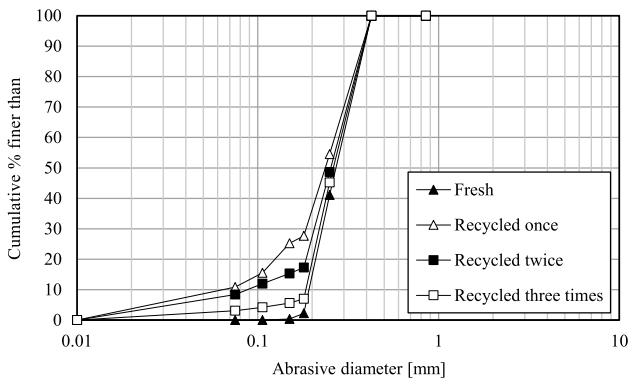
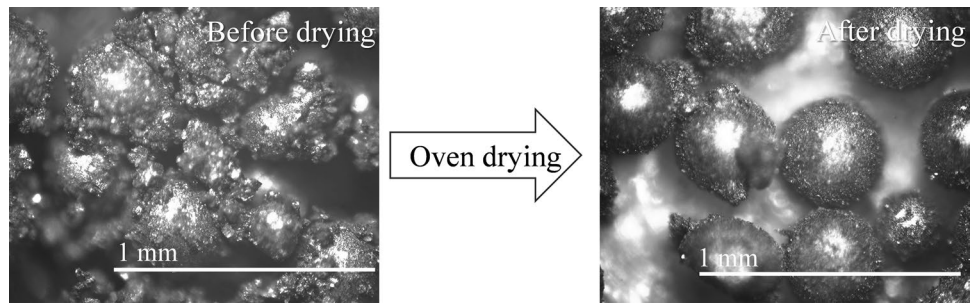
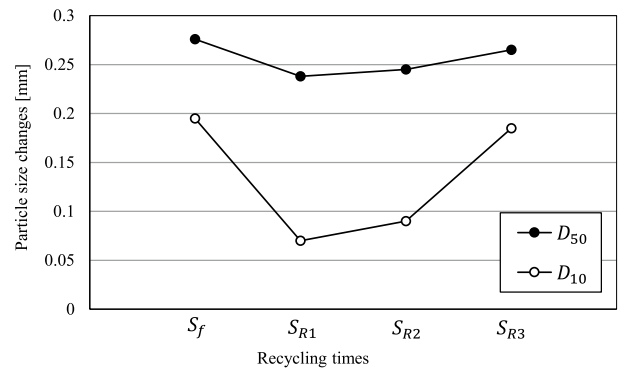


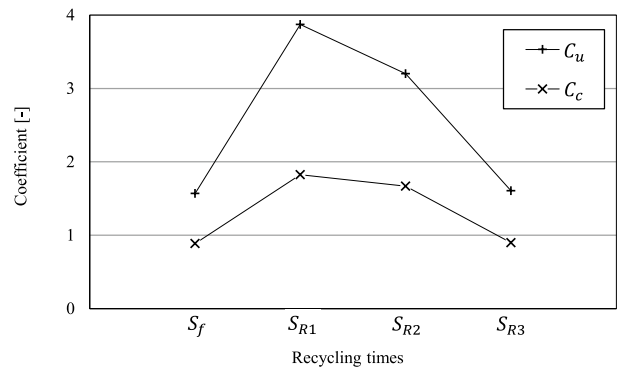
Fig. 14 Particle-size distribution

The recycled steel shot (after two runs) yielded a smaller decrease of the effective size (D_{10}) and an increase of the coefficient of gradation (C_c) compared with the recycled steel shot. This can be explained by the relatively strong steel shot left after the first recycling run. Defective or weak steel shot had already been destroyed during the primary recycling run. The recycled steel shot (after two runs) showed more rust on the particle surface. In this case, a larger amount of broken particles was observed at the mesh size 100 and 140. As a result of sieve analysis following three times of recycling of steel shots, the effective size decreased (D_{10}). The change in the coefficient of gradation (C_c) was smaller than that of the twice recycled steel shot. This can be also explained by the fact that stronger, intact particles were left. On the surfaces of these particles, more rust was found than the case of steel shot that was recycled twice. Regardless of the number of recycling runs, used steel shot retained on the mesh size 80 has its original spherical shape. In the case where three recycling times were used, the original values of the size parameters (i.e., effective and mean particle sizes) and coefficient (i.e., uniformity coefficient and coefficient of gradation) were recovered.

Figure 17 shows the cutting performance according to the drying type of the collected steel shot. As a result of the cutting experiment, the cutting performance of rapidly dried recycled steel shot (oven day) was relatively higher than that



(a) Effective size and mean particle size during recycling



(b) Uniformity coefficient and coefficient of gradation during recycling

Fig. 15 Steel ball particle-size changes as a function of the recycling times

of natural day, although no visible difference between oven dry (1 day) and natural dry (1 month) was observed.

As shown in Fig. 18, it is expected that approximately 60% of the steel shot can be recycled based on particle-size distribution and the retention of the particle shape. This result shows a higher reusability of the particles that were recycled two and three times compared with the garnet [i.e., 83%, 55%, and 31%, for one, two, and three recycling runs for garnet, respectively (Babu and Chetty 2003)]. Owing to the types of mineral composition, the steel shot maintained its original conditions compared with the garnet. Through the comprehensive analysis of these experimental results, the

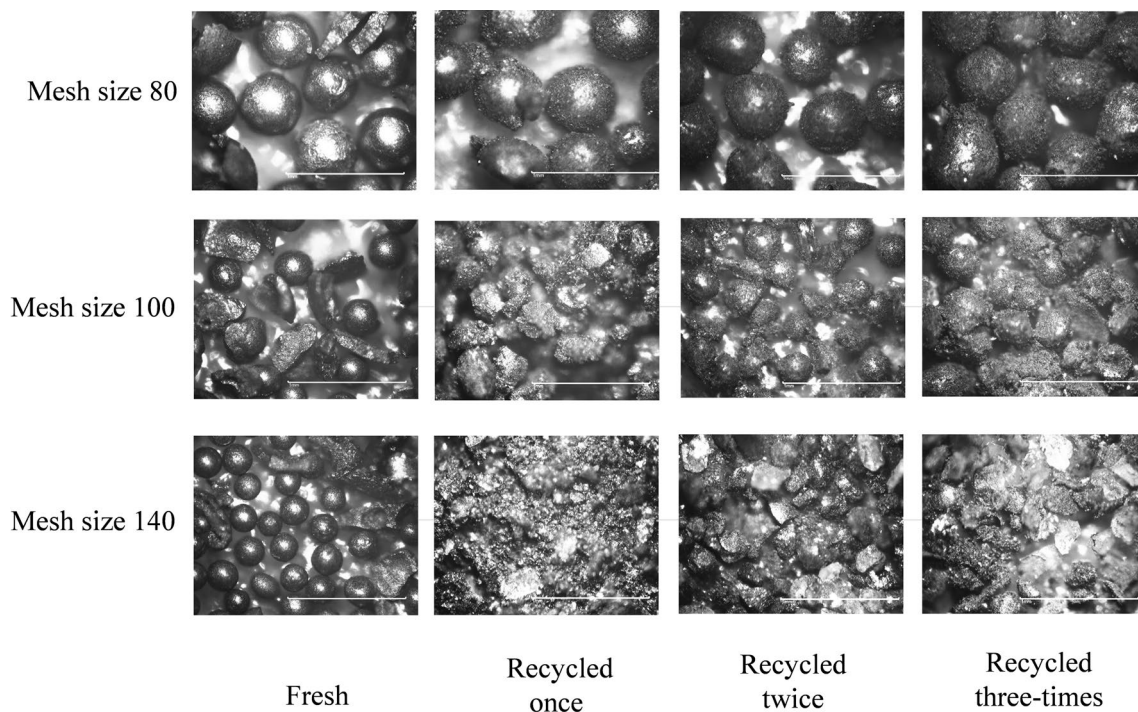


Fig. 16 Dried steel shot images at different recycling steps

following characteristics can be observed. Given that a high-hardness steel shot is more resistant to collisions, and given that it cracked compared to a low-hardness steel shot, the hardness of an abrasive is inversely proportional to its reusability. Thus, the medium hardness steel shot is suitable for recycling. Like natural garnet, the produced steel shot can also have blowhole, crack, and dendritic voids. Therefore, a more intact steel shot is suitable for recycling.

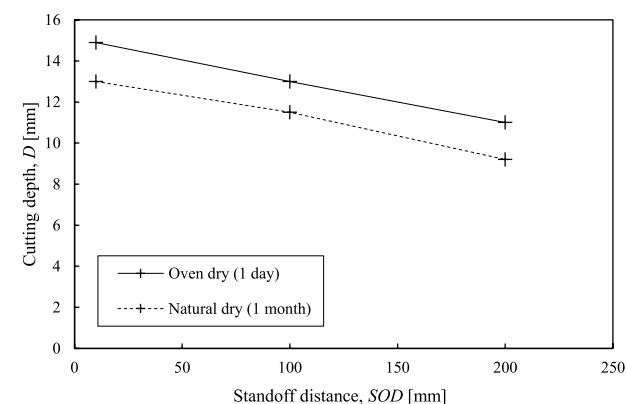
6 Conclusions

The purpose of this study was the evaluation of the performance and recycling characteristics of steel shot for rock cutting with abrasive waterjets. The cutting performance of the steel shot and the garnet depended on the abrasive waterjet parameters, such as water pressure, abrasive flow rate, traverse speed, and standoff distance, were evaluated experimentally, and the results were compared. In addition, this study aimed to identify the characteristics of steel shot recycling (up to three times) based on the analysis of the surface condition and particle-size distribution of the reused steel shot for the cutting of strong rock. The following are the major findings of this study.

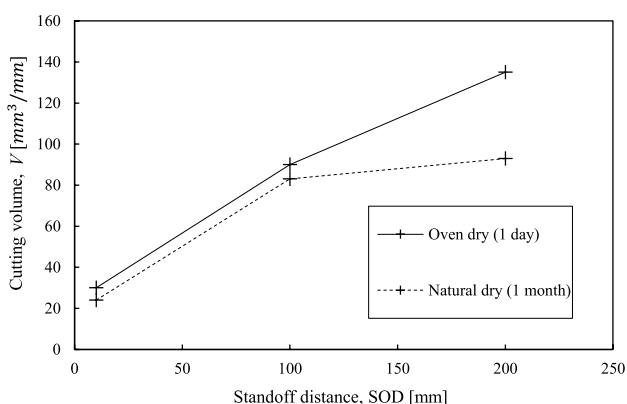
- The steel shot was typically cut by 40–50% deeper than the garnet at the same input mass. The depth of rock cutting with steel shot waterjet exhibited a general

trend, such that the cutting depth was deeper when a higher pressure, longer exposure time (slower traverse speed), and a shorter standoff distance were used. The threshold pressure (p_c) was determined based on the properties of the rock that was intended to be cut and was in the range of 80–100 MPa in both of steel shot and garnet.

- Subject to the experimental conditions, the optimum abrasive flow rate of the steel shot was approximately 12 g/s, and the normalized abrasive cutting depth changes were very similar to the results of the garnet. This result can be demonstrated as the acceleration and input energy of the abrasive as that was determined by the abrasive input mass.
- The steel shots are partially destroyed after rock cutting and most of them retained their original shape, and recycled steel shot reduced the cutting performance by 50%. This led to a cutting performance that was similar to that of the primary recycling in secondary recycling but slightly lower, owing to the increased ratio of large and intact steel shots after previous recycling.
- Steel shots had a high recycling rate of ~ 60%. Rust was observed on the recycled steel shot, and the steel shot that maintained perfect spherical shape decreased in repeated recycling runs. It is expected that the recycling rate will be increased with rapid drying and heat treatment to prevent rust and reductions in particle destruction.



(a) Depth of cut as a function of the standoff distance



(b) Volume of cut as a function of the standoff distance

Fig. 17 Effect of the drying type on the recycled steel shot waterjet rock cutting

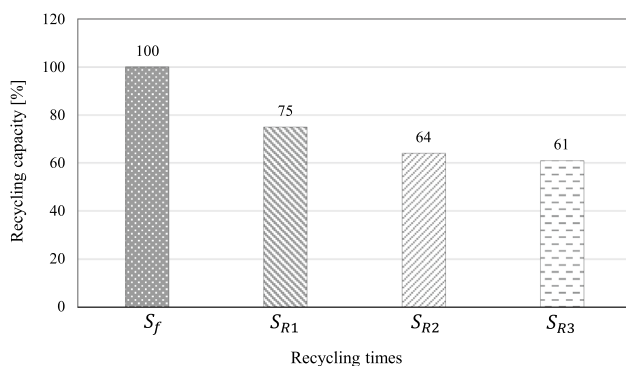


Fig. 18 Recycling rate of steel ball

Acknowledgements This work was supported by the National Research Foundation of Korea (NRF) grant funded by the Korean government (MSIT) (No. 2017R1A5A1014883) and the Basic Research Project of the Korea Institute of Geoscience and Mineral Resources (KIGAM, GP 2020-010) funded by the Ministry of Science and ICT, Korea.

Funding Not applicable.

Availability of Data and Materials Not applicable.

Code Availability Not applicable.

Compliance with Ethical Standards

Conflict of Interest The authors declare that they have no conflicts of interest.

Open Access This article is licensed under a Creative Commons Attribution 4.0 International License, which permits use, sharing, adaptation, distribution and reproduction in any medium or format, as long as you give appropriate credit to the original author(s) and the source, provide a link to the Creative Commons licence, and indicate if changes were made. The images or other third party material in this article are included in the article's Creative Commons licence, unless indicated otherwise in a credit line to the material. If material is not included in the article's Creative Commons licence and your intended use is not permitted by statutory regulation or exceeds the permitted use, you will need to obtain permission directly from the copyright holder. To view a copy of this licence, visit <http://creativecommons.org/licenses/by/4.0/>.

References

- ASTM (2007) D422-63: standard test method for particle-size analysis of soils. ASTM International West Conshohocken
- ASTM (2009) D6913-04: Standard test methods for particle size distribution (gradation) of soils using sieve analysis ASTM International West Conshohocken
- ASTM (2014) D7012-14: Standard test method for compressive strength and elastic moduli of intact rock core specimens under varying states of stress and temperatures, ASTM International, West Conshohocken, Pa., doi ASTM International West Conshohocken
- Ay M, Çaydaş U, Haşçalık A (2010) Effect of traverse speed on abrasive waterjet machining of age hardened Inconel 718 nickel-based superalloy. *Mater Manuf Process* 25:1160–1165
- Aydin G (2014) Recycling of abrasives in abrasive water jet cutting with different types of granite. *Arab J Geosci* 7:4425–4435
- Aydin G (2015) Performance of recycling abrasives in rock cutting by abrasive water jet. *J Central South Univ* 22:1055–1061
- Babu MK, Chetty OK (2002) Studies on recharging of abrasives in abrasive water jet machining. *Intern J Adv Manuf Technol* 19:697–703
- Babu MK, Chetty OK (2003) A study on recycling of abrasives in abrasive water jet machining. *Wear* 254:763–773
- Brown ET (1981) *Rock characterization testing and monitoring*. Pergamon Press, UK
- Capello E, Groppetti R (1993) On a simplified model for hydro abrasive jet machining prediction, control and optimization. In: *Proceedings of the 7th American Water Jet Conference*, pp. 157–174
- Cha Y, Oh T-M, Cho G-C (2019) Waterjet erosion model for rock-like material considering properties of abrasive and target materials. *Appl Sci* 9:4234. <https://doi.org/10.3390/app9204234>
- Cha Y, Oh T-M, Cho G-C (2020) Effects of focus geometry on the hard rock-cutting performance of an abrasive waterjet. *Adv Civil Eng* 2020:1–13
- Chetty O, Babu R (1999) Some investigations on abrasives in abrasives waterjet machining. In: *Proceeding of 10th American waterjet*

- conference, Waterjet Technology Association, USA, 1999. pp 419–430
- Daniewicz S, Cummings S (1999) Characterization of a water peening process
- El-Domiati A, Abdel-Rahman A (1997) Fracture mechanics-based model of abrasive waterjet cutting for brittle materials. *Intern J Adv Manuf Technol* 13:172–181
- Evans AG, Gulden M, Rosenblatt M (1978) Impact damage in brittle materials in the elastic-plastic response regime. *Proc R Soc Lond A Math Phys Sci* 361:343–365
- Finnie I (1960) Erosion of surfaces by solid particles. *Wear* 3:87–103
- Fowler G, Pashby IR, Shipway PH (2009) The effect of particle hardness and shape when abrasive water jet milling titanium alloy Ti6Al4V. *Wear* 266:613–620. <https://doi.org/10.1016/j.wear.2008.06.013>
- Galecki G, Summers D (1992) Steel shot entrained ultra high pressure waterjet for cutting and drilling in hard rocks. *Jet cutting technology*. Springer, Berlin, pp 371–388
- Guo N, Louis H, Meier G, Ohlsen J (1992) Recycling capacity of abrasives in abrasive water jet cutting. *Jet cutting technology*. Springer, Berlin, pp 503–523
- Hascalik A, Çaydaş U, Gürün H (2007) Effect of traverse speed on abrasive waterjet machining of Ti-6Al-4V alloy. *Mater Design* 28:1953–1957
- Hashish M (1989) A model for abrasive-waterjet (AWJ). *Mach J Eng Mater Technol* 111:154–162. <https://doi.org/10.1115/1.3226448>
- Hashish M (2011) AWJ cutting with reduced abrasive consumption. In: *Proceeding of the American Water Jet Conference*, Houston, USA, Paper A
- Jankovic P, Igetic T, Nikodijevic D (2013) Process parameters effect on material removal mechanism and cut quality of abrasive water jet machining. *Theoret Appl Mech* 40:277–291. <https://doi.org/10.2298/tam1302277j>
- Maurer WC, Joe KH (1969) Hydraulic jet drilling. *Soc Petrol Eng AIME Paper No SPE 2434*:213–224
- Momber A (2001) Stress–strain relation for water-driven particle erosion of quasi-brittle materials. *Theor Appl Fract Mech* 35:19–37
- Momber AW (2004) Wear of rocks by water flow. *Int J Rock Mech Min Sci* 41:51–68. [https://doi.org/10.1016/s1365-1609\(03\)00075-3](https://doi.org/10.1016/s1365-1609(03)00075-3)
- Momber A, Kovacevic R (1995) Energy dissipative processes in high speed water-solid particle erosion. *Asme-Publications-Htd* 321:555–564
- Momber AW, Kovacevic R (2012) *Principles of abrasive water jet machining*. Springer Science & Business Media, Germany
- Oh T-M, Cho G-C (2013) Characterization of effective parameters in abrasive waterjet rock cutting. *Rock Mech Rock Eng* 47:745–756. <https://doi.org/10.1007/s00603-013-0434-3>
- Oh T-M, Cho G-C (2015) Rock cutting depth model based on kinetic energy of abrasive waterjet. *Rock Mech Rock Eng* 49:1059–1072. <https://doi.org/10.1007/s00603-015-0778-y>
- Perec A (2017) Disintegration and recycling possibility of selected abrasives for water jet cutting. *Dyna* 84:249–256
- Pi VN (2008) Performance enhancement of abrasive waterjet cutting
- Pi VN, Chau HV, Hung TQ (2013) A study on recycling of supreme garnet in abrasive waterjet machining. In: *Applied mechanics and materials*. Trans Tech Publ, pp 499–503
- Salko D (1984) Peening by water. In: *Second International Conference on Shot Peening (ICSP)*, Chicago, NJ, May, 1984. pp 14–17
- Summers DA (2003) *Waterjetting technology*. CRC Press, USA
- Vahedi Tafreshi H, Pourdeyhimi B (2003) The effects of nozzle geometry on waterjet breakup at high Reynolds numbers. *Exp Fluids* 35:364–371. <https://doi.org/10.1007/s00348-003-0685-y>
- Zeng J, Kim TJ (1992) Development of an abrasive waterjet kerf cutting model for brittle materials. *Jet cutting technology*. Springer, Berlin, pp 483–501
- Zeng J, Kim TJ (1996) An erosion model of polycrystalline ceramics in abrasive waterjet cutting. *Wear* 193:207–217
- Zhu HT, Huang CZ, Wang J, Zhao GQ, Li QL (2009) Modeling material removal in fracture erosion for brittle materials by abrasive waterjet. In: *Advanced Materials Research*. Trans Tech Publ, pp 357–362

Publisher's Note Springer Nature remains neutral with regard to jurisdictional claims in published maps and institutional affiliations.